Available online at www.sciencedirect.com
ScienceDirect
Journal of Hazardous Materials 159 (2008) 158–168
Journal of Hazardous Materials
www.elsevier.com/locate/jhazmat

Application of CFD (Fluent) to LNG spills into geometrically complex environments

Filippo Gavelli [a,*], Edward Bullister [b], Harri Kytomaa [a]

[a] *Exponent, Inc., 17000 Science Drive, Suite 200, Bowie, MD 20715, United States*
[b] *Cambridge Technology Development, Inc., United States*

Received 4 February 2008; accepted 5 February 2008
Available online 17 February 2008

Abstract

Recent discussions on the fate of LNG spills into impoundments have suggested that the commonly used combination of SOURCE5 and DEGADIS to predict the flammable vapor dispersion distances is not accurate, as it does not account for vapor entrainment by wind. SOURCE5 assumes the vapor layer to grow upward uniformly in the form of a quiescent saturated gas cloud that ultimately spills over impoundment walls. The rate of spillage is then used as the source term for DEGADIS. A more rigorous approach to predict the flammable vapor dispersion distance is to use a computational fluid dynamics (CFD) model. CFD codes can take into account the physical phenomena that govern the fate of LNG spills into impoundments, such as the mixing between air and the evaporated gas. Before a CFD code can be proposed as an alternate method for the prediction of flammable vapor cloud distances, it has to be validated with proper experimental data.

This paper describes the use of Fluent, a widely-used commercial CFD code, to simulate one of the tests in the "Falcon" series of LNG spill tests. The "Falcon" test series was the only series that specifically addressed the effects of impoundment walls and construction obstructions on the behavior and dispersion of the vapor cloud. Most other tests, such as the Coyote and the Burro series, involved spills onto water and relatively flat ground. The paper discusses the critical parameters necessary for a CFD model to accurately predict the behavior of a cryogenic spill in a geometrically complex domain, and presents comparisons between the gas concentrations measured during the Falcon-1 test and those predicted using Fluent. Finally, the paper discusses the effect vapor barriers have in containing part of the spill thereby shortening the ignitable vapor cloud and therefore the required hazard area. This issue was addressed by comparing the Falcon-1 simulation (spill into the impoundment) with the simulation of an identical spill without any impoundment walls, or obstacles within the impoundment area.

Keywords: LNG; LNG hazard; Spills; Vapor dispersion; CFD; Impoundment

1. Background and motivation

Natural gas demand has been rapidly growing worldwide over the past few years, leading to a large number of applications for the siting, construction and operation of new LNG receiving terminals, particularly in Europe and North America. Currently there are approximately 40 new LNG receiving terminals either in construction or in the permitting process in North America alone, and approximately 20 additional potential sites are being considered. The growing interest in LNG and the potential for some of the new terminals to be located in proximity of highly populated areas has raised questions about the safety of LNG transportation and regasification.

An important element of the overall risk assessment of LNG operations is the definition of the hazard footprint—the area, centered around the LNG terminal, within which hazardous conditions may be present in the event of an LNG spill. The hazardous conditions of interest for public safety are: (1) radiant heat flux from an LNG pool fire; and (2) the potential for a flammable vapor cloud from an LNG spill to reach a remote ignition source and result in a flash fire. Federal regulations (49 CFR 193) require that applications for land-based (onshore) LNG receiving terminals demonstrate that the hazards created by an LNG spill will not extend beyond the area under the control of the terminal operator.

In this paper, we address the dispersion of a flammable vapor cloud following a spill of LNG into an impoundment. To date, the modeling tools used to estimate the dispersion of vapors emanating from an LNG spill have mostly been limited to integral-type

* Corresponding author. Tel.: +1 301 291 2512; fax: +1 301 291 2599.
E-mail address: fgavelli@exponent.com (F. Gavelli).

0304-3894/$ – see front matter © 2008 Elsevier B.V. All rights reserved.
doi:10.1016/j.jhazmat.2008.02.037

models (e.g., DEGADIS [1]), whose assumptions limit their use to dispersion over flat terrain or water. Typically, the calculation of flammable vapor dispersion hazard distances for LNG spills into impoundments utilizes DEGADIS together with another integral-type model (SOURCE5). Given the LNG spill flow rate and the size and materials of the impoundment, SOURCE5 calculates the time-dependent volume occupied by the natural gas (the sum of the residual LNG volume and the volume of gas produced by vaporization of the LNG), and compares it to the volume of the impoundment. When the combined volume of LNG and saturated vapor in the impoundment exceeds the volume of the impoundment, the excess vapor is considered to be released out of the impoundment and becomes a source term for DEGADIS, which calculates its dispersion.

Recent discussions in the LNG safety debate have pointed out some limitations in the SOURCE5 model, namely its inability to account for the expansion of the vapor volume due to heating above the boiling temperature of LNG, as well as its inability to account for mixing between the rising vapor cloud within the impoundment and the wind over the impoundment walls. Consequently, the Federal Energy Regulatory Commission (FERC) has taken the conservative position that the use of SOURCE5 to quantify the LNG vapor source term for use in DEGADIS, in the context of design spills into an impoundment, is inadequate. FERC has recently required at least two applicants [2] to revise their flammable vapor cloud dispersion calculations and not to take credit for any vapor holdup within the impoundment. The result of this artificial approach is a hazard distance (distance to 1/2 LFL) that greatly exceeds previous calculations. The new requirement, while certainly conservative, puts a heavy and unnecessary burden on the industry: in order to prevent the flammable vapor loud from extending beyond the plant's boundaries, applicants need to either relocate the LNG storage tanks or construct deep sumps to the LNG spill impoundments.

An alternative to the no-vapor-holdup approach is to use modeling tools that can account for all the physical phenomena that affect the vapor outflow from an impoundment. Several computational fluid dynamics (CFD) programs are currently available to the industry for this very purpose. CFD techniques are increasingly being applied to model environmental source and dispersion problems. CFD models based upon the underlying principles of fluid dynamics that govern the physics of the flow problem. Advances in the speed of modern computers, and more significant recent advances in CFD techniques, have made CFD modeling tractable for complex environmental problems such as LNG spills. The use of CFD for the simulation of LNG vapor cloud dispersion is strongly recommended by the Sandia National Laboratories 2004 report [3]. Before a CFD model can be used for this purpose, however, it must be validated against relevant experimental data, to ensure that the vapor dispersion predictions are sufficiently accurate.

When considering spills into an impoundment, as opposed to spills over water or flat terrain, it is important to consider the effect on vapor dispersion and mixing due to the impoundment walls and the LNG storage tank or process equipment within the impoundment. Only one series of large-scale LNG spill tests has been performed, in which the effect of these obstacles was taken into account: the Falcon test series. It must be noted that the Falcon test series consisted of LNG spills onto a water pond, not on land. The different substrate affects the rate of LNG vapor formation, but not the vapor holdup effect of the impoundment walls; therefore, the Falcon test series is a valid data set for this study. This paper discusses the validation of Fluent, the most commonly-used commercial CFD package in the world, against data from the Falcon test series.

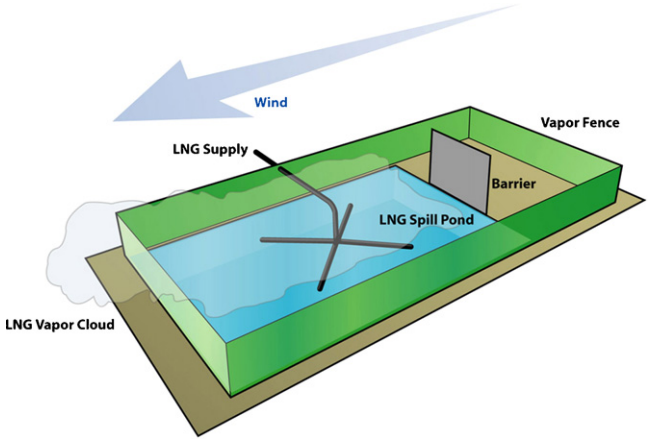

Fig. 1. Artist rendition of the Falcon test pond and impoundment area.

2. The Falcon test series

The Falcon test series consists of five large-scale LNG spill tests conducted by Lawrence Livermore National Laboratories in 1987, in the Frenchman Flat area, in Nevada [4]. These tests were specifically aimed at evaluating the effectiveness of impoundment walls as a mitigation technique for accidental releases of LNG, and to provide experimental data for the validation of computer models. LNG was spilled onto a rectangular water pond (60 m long and 40 m wide), equipped with a water recirculation system to maximize evaporation of the spilled LNG, so that the evaporation rate would be approximately equal to the spill flow rate. To this end, LNG was introduced through 4 pipes, fitted with 0.11 m diameter orifices and spaced at 90° intervals (the spill "spider") to maximize the size of the LNG pool onto the water surface (Fig. 1 shows an artist rendition of the Falcon test rig). The vapor fence, approximately 8.7 m high, extended upwind of the water pond, enclosing a total area 44 m wide × 88 m long. In addition to the fence, a 13.3 m tall billboard, 17.1 m wide, was located just upwind of the water pond. The purpose of the billboard was to simulate the effect of a storage tank or other obstruction on the dispersion of the vapor cloud. The terrain surrounding the fenced area was flat and the experiments were performed under stable or neutrally stable atmospheric stability conditions (Pasquill-Gifford classes D–F). The total volume of spilled LNG was such that the corresponding volume of saturated vapor was less than the volume of the impoundment.

The Falcon tests were heavily instrumented to measure the following quantities: air temperature, pressure and humidity, wind speed and direction, turbulence intensity, heat flux from

the ground, and gas concentration. The sensors were located both within the fenced area, to record the behavior of the constrained LNG cloud, and downwind of the fence, to observe the dispersion of the LNG vapor that spilled over the fence. Sensors were located up to 250 m downwind of the trailing edge of the vapor fence.

Several aspects of these tests are desirable for validating a CFD model for LNG spills:

- These tests used a realistically complex geometry that represents conditions likely to be present at or near an LNG release. The vapor fence simulates the effect of the impoundment walls, and the barrier was placed upwind of the spill to introduce additional turbulence, in a manner similar to the effect that containment tanks, buildings or even ships would have on an actual spill. These types of surface features and realistic flow complexity test the capability of the CFD model to accurately predict dispersion in the flow patterns formed in complex geometries.
- A predetermined amount of LNG was spilled into an impoundment at a prescribed rate, and the flammable vapor cloud was then tracked as it was carried downwind and dispersed in the environment. Therefore, the Falcon tests provide data on the entire LNG vapor cloud dispersion scenario.
- The LNG spill was set up in a repeatable manner, with a well-defined vapor source term. For modeling purposes, this allows the vapor source term to be prescribed in the CFD model with minimal uncertainties.
- These tests included detailed and redundant instrumentation, and measured several quantities of interest that can be directly compared with the CFD model predictions. The array of measurement stations was distributed appropriately in the region adjacent to and downwind of the spill.

3. Fluent

Fluent is a general purpose CFD code that has been in use since 1983 and has been applied to a broad range of disciplines (e.g., aerospace, chemical, environmental, etc.). The authors are not developers nor distributors of the Fluent software package. Fluent was used for this study only due to the authors' familiarity with the code and to its applicability to this type of analysis.

The core Fluent solver has been validated for a large number of industrial problems and with thousands of academic papers. One example of pertinent work is a recent paper about the use of Fluent by the Environmental Protection Agency to analyze the dispersion of plumes in the atmosphere under various atmospheric stability criteria [5]. In another paper, Savvides et al. [6] present a study validating the Fluent code against the experimental results of Cleaver et al. [7,8].

Fluent is especially appropriate for the complex physics involved in an LNG spill for several reasons. First, Fluent has a very well developed atmospheric dispersion model, which uses the Reynolds stress turbulence model for independent calculation of the turbulent viscosity in the vertical and horizontal directions. Fluent gives programming access to the core of the computational solver through user-defined functions. This provides the flexibility to customize the model to the wide range of physics involved in the problem.

3.1. Fluent CFD solver

The Fluent software solves the Navier–Stokes equations for gas flow, coupled with the energy and diffusion equations. Fluent simulates the gas mixture by modeling each chemical species independently. For details on the Fluent solver, the reader is referred to the company's website (http://www.fluent.com). For this study, the low Mach number incompressible ideal gas solver was specified: gas density is allowed to vary as a function of local temperature and chemical composition, according to the ideal gas law, but does not depend on the local pressure.

3.2. Turbulence modeling

Turbulence was modeled using the k–ε model [9] in conjunction with the Reynolds stress model (RSM) [10]. The standard k–ε model generates a single, isotropic "eddy viscosity". The standard k–ε (without Reynolds stress calculation) tends to be ill-suited for this type of atmospheric problem because it overpredicts the generation of turbulent kinetic energy (TKE) in a normal boundary layer where the wind impinges on a structure, and this excess TKE is convected downwind to further contaminate the calculation. It is also critical that the turbulence model take into account the stabilizing effects of density that varies with height. The RSM involves calculation of the individual Reynolds stresses using differential transport equations. The RSM adds accuracy to the k–ε model, at the expense of stability. Therefore, the k–ε model was used to generate an approximate solution of the turbulence, which would serve as the initial guess for the RSM model.

4. Modeling approach

The analysis presented in this paper focuses on the simulation of the Falcon-1 test. This test was chosen as the benchmark case as it combines low wind speed conditions (1.7 m/s at 2 m elevation) with other challenging conditions from an analysis standpoint among the Falcon tests: most stable atmosphere, largest spill volume (66.4 m^3) and spill flow rate (28.7 m^3/min). In low winds and a stably stratified atmosphere, the plume does not readily mix with the wind to dilute the gas concentration below the lower flammability limit (LFL). These conditions are of interest in plume dispersion studies as they constitute the worst case scenario for the spread of the flammable plume.

Also of interest is the fact that, if the SOURCE5/DEGADIS model is applied to the Falcon-1 spill, the vapor cloud would be predicted to remain confined inside the vapor fence, unlike what was observed during the experiment. Therefore, any model that can accurately simulate the Falcon-1 test data must be able to account for physical phenomena other than vaporization, in order for the cloud to overflow the impoundment and disperse downwind.

4.1. Computational geometry and grid

The domain is oriented such that the *X*-direction is horizontal and parallel to the wind, the *Y*-direction is horizontal and perpendicular to the wind, and the *Z*-direction is vertical. The origin of the reference frame is placed at ground level, on the downwind fence along the plane of symmetry of the impoundment. The computational domain extended 500 m in the *X*-direction (from 200 m upwind to 300 m downwind of the vapor fence trailing edge) and 500 m in the *Y*-direction (crosswind). The top of the computational domain was located at a nominal height of $Z = 50$ m at $X = 0$ m and grew slowly in the *X*-direction, to allow a small component of the horizontal wind velocity at the top boundary to enter the computational domain.

The computational domain was discretized using hexahedral (brick) elements. The hexahedral meshes are much more computationally efficient than tetrahedral meshes. Typically, a hexahedral mesh requires half the resolution in each of the three directions, for almost an order of magnitude reduction in the number of elements. Tetrahedral elements can be used in portions of the geometry that are too complex to easily discretize with hexahedral elements. The solution is then calculated on the hybrid tetrahedral–hexahedral mesh. This allows solution of problems in arbitrarily complex geometries while realizing the high efficiency of hexahedral elements.

Further gains in computational efficiency were realized by aligning the local coordinate system of the computational elements with the predominant wind direction in the atmospheric boundary layer. Finally, a non-uniform mesh was adopted, to accommodate the features of the flow field; a finer mesh was used in regions of high flow gradients, such as near the billboard and vapor fence (Fig. 2).

4.2. Boundary conditions and initial conditions

The planetary boundary layer wind profile was specified as a velocity inlet boundary condition at the upwind boundary and at the top of the computational domain. The values for velocity, temperature, and turbulent kinetic energy and dissipation were calculated as a function of height from the Monin–Obukov equations that were fit to the wind data in the Falcon test report [4] for the Falcon-1 test. The direct calculation from the wind velocity yielded $U^* = 0.11$ m/s, $T^* = 0.577$ K and $L = 11$ m. For computational efficiency, the side boundaries of the computational domain were aligned parallel to the average measured wind direction, which was at an angle of -9.3° with respect to the alignment of the fence. Symmetry boundary conditions were imposed along the side boundaries, which is consistent with and representative of these surfaces being parallel to the wind direction. A pressure outlet boundary condition was imposed at the downwind boundary. A wall boundary condition was applied to the ground, with a surface roughness value of 0.16 m inferred from the wind profile.

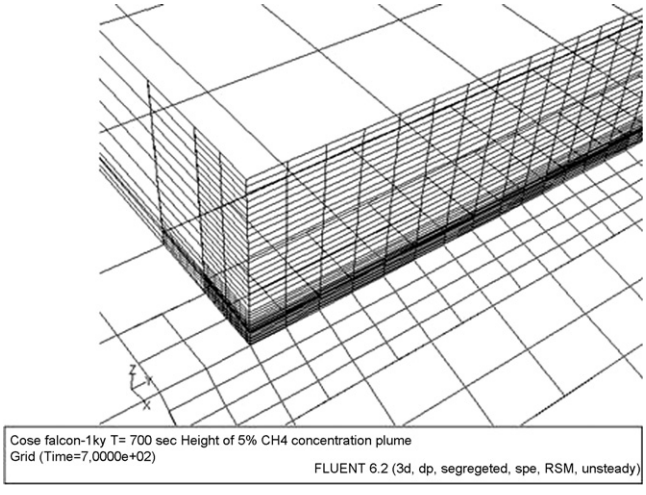

Fig. 2. Non-conforming hexahedral mesh locally refined near the downwind fence.

For the duration of the spill (131 s in the case of Falcon-1), an inlet velocity boundary condition was applied for the gas entering the domain over the water pond area. The injected gas temperature was set equal to the boiling temperature of LNG (111 K). The flow rate and total volume of gas introduced were consistent with the experimental data for the Falcon-1 test. The reported LNG vaporization rates for spills on water varied between approximately 0.029 and 0.195 kg/m^2 s [11]. For this study, an LNG mass flux rate of 0.12 kg/m^2 s was assumed, as estimated during the Avocet tests [12]; this vaporization rate corresponds to an upward flow velocity of saturated methane gas of 44 mm/s directed into the domain from the pool surface.

The spill spider for the injection of LNG was intended to allow LNG to spread across the full area of the pool and vaporize uniformly and quickly over the pool surface. Estimates based on the analysis of video recordings of the Falcon tests indicated that the LNG pool spread to the entire water pond surface within approximately 6–10 s after the spill started. Initially, the simplifying assumption was made that the LNG pool immediately covered the entire water pond. This assumption resulted in an overprediction of the LNG vapor generation rate during the early phase of the test.

The high LNG velocity (approximately 6.3 m/s radially at the injection points) introduces a level of turbulence that is significant, compared to the otherwise quiescent air within the vapor fence. Direct observation of the development of the plume from the LNG spill, from videos of the Falcon test series, indicates that the LNG impacting the water pond surface rapidly forms a plume of approximately 2 m in height. The fluctuating velocity component associated with the plume was estimated to be approximately 3 m/s. Based on this, the inlet turbulent kinetic energy (K) for the k–ε model was estimated to be 9 m^2/s^2. The inlet value for ε was calculated from K and from the observed length scale $L_e = 2$ m of the largest energy-containing eddies from the formula [13]:

$$\varepsilon = \frac{C_\mu^{3/4} K^{3/2}}{L_e} \tag{1}$$

where $C_\mu = 0.09$. For different LNG velocities, the fluctuating speed would be expected to scale linearly with the nozzle exit velocity, and K would scale as the square of the nozzle exit

velocity. These values of K and ε were imposed on both the pool inlet boundary conditions and in the observed 2 m layer immediately above the pool surface. At all other locations, all quantities were calculated from the flow equations.

These conditions were maintained for the duration of the spill. At the end of the spill, the turbulence of the entering gas was disabled and the pond was changed to a wall boundary condition, with temperature equal to the measured post-spill pool temperature (22.4 °C).

4.3. Solution method

Height-dependent velocity, temperature, and turbulence intensity were specified throughout the domain as initial conditions, according to the Monin–Obukhov equations. A steady-state solution was first sought for the air velocity field, prior to the injection of natural gas, by implementing the standard k–ε model to get the solution within the convergence radius of the RSM model, and then switching to the more accurate (but less stable) RSM. This established the ambient conditions before the spill was initiated at time $t = 0$.

A time-dependent simulation was then performed. At time $t = 0$, natural gas was injected into the domain by changing the water pond boundary condition from a "solid wall" boundary (i.e., no flow of air or LNG vapor is allowed in or out of the domain across the water surface) to an "inlet flow" boundary (i.e., LNG vapors are injected into the domain, at a specified rate, through the water pond surface). The inlet flow boundary condition was maintained for the duration of the spill (131 s). The water pond surface then reverted back to a solid wall boundary for the remainder of the transient simulation (up to 700 s).

Three different cases were considered for the Falcon-1 test simulation:

(1) The baseline case, which replicated the geometry, initial and boundary conditions of the Falcon-1 test.
(2) A no-barriers case, in which the baseline setup was repeated but the fence and billboard were removed.
(3) A no-source-turbulence case, in which the baseline setup was repeated but the turbulence associated with the injection and vaporization of LNG was set to zero, which is the inherent assumption that is made by SOURCE5.

5. Results

5.1. Baseline case—velocity profiles at inlet boundary and downwind

The Monin–Obukov equations were used to generate the initial inlet velocity and temperature profiles. Fig. 3 shows the evolution of the velocity profile through the domain, prior to injecting LNG. The profiles are taken at points offset from the domain's midplane, to avoid any wake effects from the impoundment. The plot shows that the desired velocity profile is sustained, almost unaltered, throughout the computational domain, and therefore the LNG spill occurs in the correct environment.

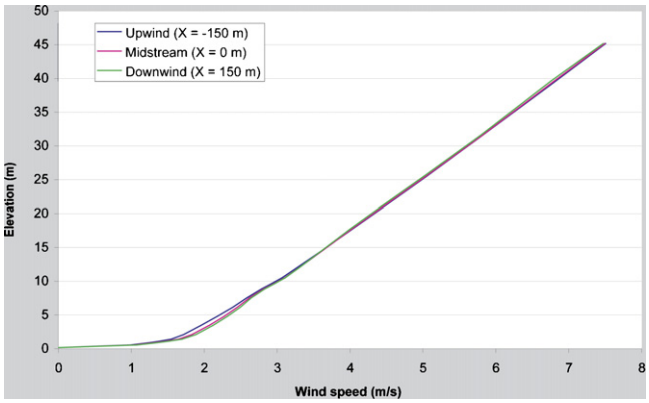

Fig. 3. Velocity profile at inlet boundary and various downwind locations, prior to the release of LNG.

Fig. 4 compares the undisturbed velocity profile (near the inlet boundary) with the velocity profile in the wake of the impoundment, in the presence of the vapor cloud. The presence of the vapor cloud is noticeable at low elevations: the slumping behavior of the dense cloud increases the local air velocity well above the initial conditions.

5.2. Comparison of baseline run with experimental data

The Falcon tests gas concentration data was averaged over 5 s time intervals. The CFD tool used for this study is a Reynolds-Averaged Navier–Stokes (RANS) based model and, as such, predicts a smoother and more slowly-changing behavior of the methane cloud. The averaging time for a RANS-based model, for this type of scenario, was estimated by the authors as approximately 30–60 s. The difference in averaging times between the experimental data and the CFD simulation needs to be taken into consideration when comparing the two data sets.

Figs. 5 and 6 show comparisons, at different times from the start of the LNG spill, between experimental and simulated gas concentration contours at a plane perpendicular to the wind direction, located 150 m downwind from the impoundment. The color contour map is sized to match the physical dimensions as the graphical representations of the Falcon data.

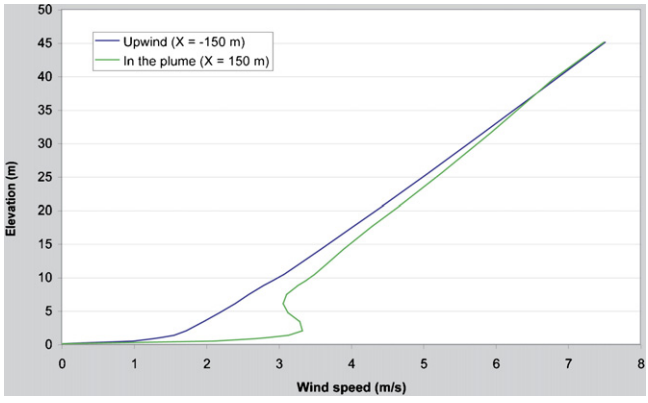

Fig. 4. Velocity profile at inlet boundary and in the presence of the vapor cloud.

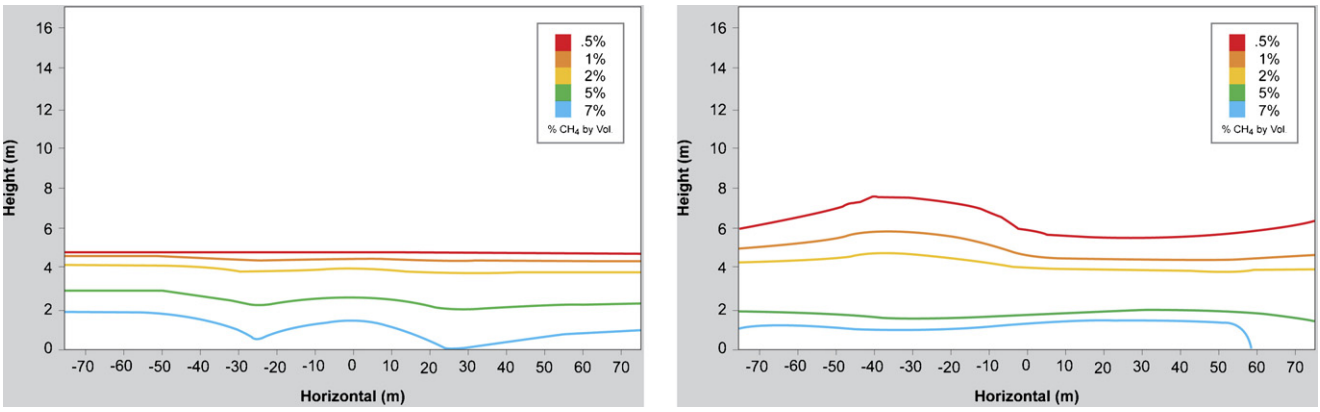

Fig. 5. Experimental (left) vs. predicted (right) gas concentration contours at plane 150 m downwind of impoundment, 200 s after spill start.

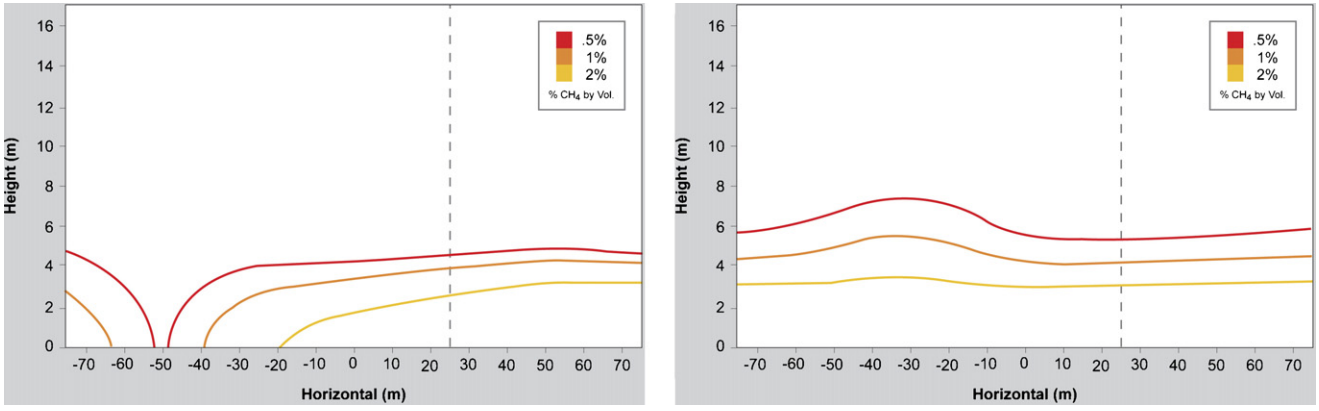

Fig. 6. Experimental (left) vs. predicted (right) gas concentration contours at plane 150 m downwind of impoundment, 280 s after spill start. The gray lines show the location sampled to obtain vertical concentration profiles (Fig. 7).

The general shape of the predicted cloud captures the stable stratification that was measured in the experimental data. The flammable clouds are approximately 5–6 m high in both cases. Minimum gas concentration occurs directly downwind of the impoundment, where the wake effect is most pronounced.

Fig. 7 shows a snapshot of the vertical gas concentration profiles (predicted by Fluent vs. measured experimentally) at a location 150 m downwind of the impoundment and +25 m crosswind of the midplane. The plot shows excellent agreement between the predicted gas concentration profile and the data points obtained from the Falcon-1 contour plot on the 150 m instrumentation plane.

Figs. 8 and 9 compare, respectively, the evolution of the predicted and measured gas concentration and air temperature at a location 150 m downwind of the impoundment, slightly off-center (25 m) with respect to the walls of the impoundment. The results show that the Fluent simulation captures the general behavior of the vapor cloud, albeit with some discrepancies. The gas concentration plot (Fig. 8) shows that the CFD-predicted vapor cloud concentration peaks at a lower value and at a later time than was measured during the experiment. The CFD-predicted vapor cloud concentration then becomes higher than the experimental data, and remains higher for the remainder of the simulation. The temperature plot (Fig. 9) shows a similar trend: in the CFD simulation, the coldest temperature reaches the sensor approximately 50 s later than during the experiment. The simulation then predicts the temperature to remain lower than measured during the experiment, indicating the presence of a higher concentration vapor cloud.

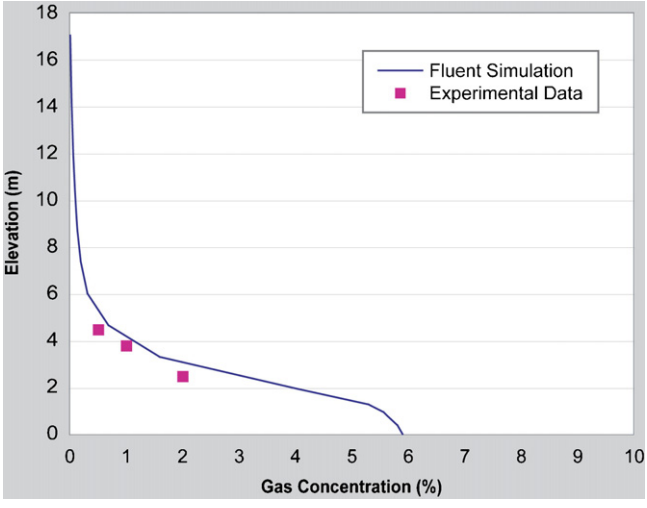

Fig. 7. Vertical concentration profiles (predicted vs. measured) at a location 150 m downwind and +25 m crosswind of the impoundment, 280 s after spill start. Experimental data is based on a 5-s time average; the simulated data is representative of approximately a 30–60 s time average.

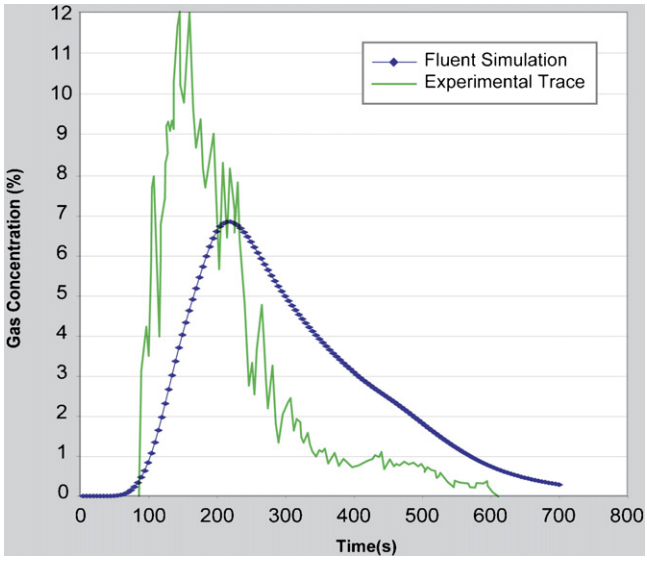

Fig. 8. Predicted vs. measured gas concentration at a location 150 m downwind of impoundment and 1 m above ground.

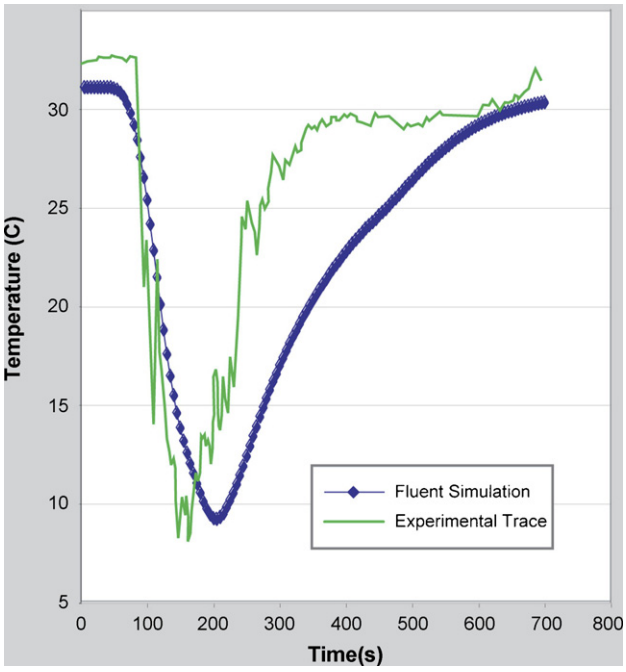

Fig. 9. Predicted vs. measured air temperature at a location 150 m downwind of impoundment and 1 m above ground.

An analysis of the gas concentration and temperature traces at several sensor locations suggests that the CFD-predicted vapor cloud overflows the impoundment later than during the experiment, and does so at a slower rate, resulting in a longer, lower concentration vapor cloud dispersing downwind. Based on this analysis, the authors believe that additional mixing of the cloud inside the impoundment would tend to improve the numerical prediction.

5.3. *Effect of impoundment*

The spill simulation was repeated without the fence that forms the perimeter of the impoundment and without the billboard that generates turbulence within the impoundment. Figs. 10–14 compare the footprint of the flammable vapor cloud from the baseline (left) and no-barriers case (right), at different times from the start of the LNG spill. The top-down views show the horizontal reach of the flammable cloud in the two cases, color-coded by the maximum height of the cloud at any given location.

In the absence of impoundment walls, the dense plume is weakly affected by the wind, and can even travel faster than the wind. This is because the dense plume forms a layer close to the ground where the wind velocity is smallest and its motion is driven by the density difference between the plume and ambient air. This is why the plume also spreads upwind and sideways.

The sequence of plots shows that the impoundment partially contains the spill and limits its spread in both the downwind and lateral directions. In fact, Fig. 11 shows that after only 50 s from the start of the spill, the unconfined vapor cloud has already extended approximately 150 m downwind of the water pond, whereas the confined cloud is still mostly contained within the vapor fence.

After the LNG spill has ended, the unconfined cloud rapidly moves away from the water pond (Fig. 14) and is convected

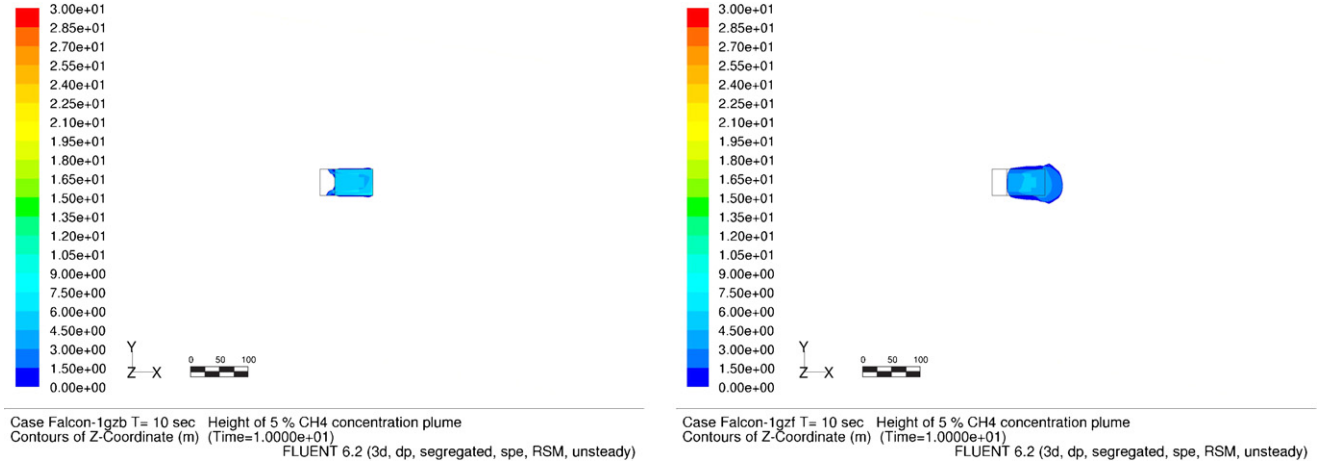

Fig. 10. Footprint of the flammable vapor cloud 10 s after the start of the spill (left = baseline case, right = no-barrier case).

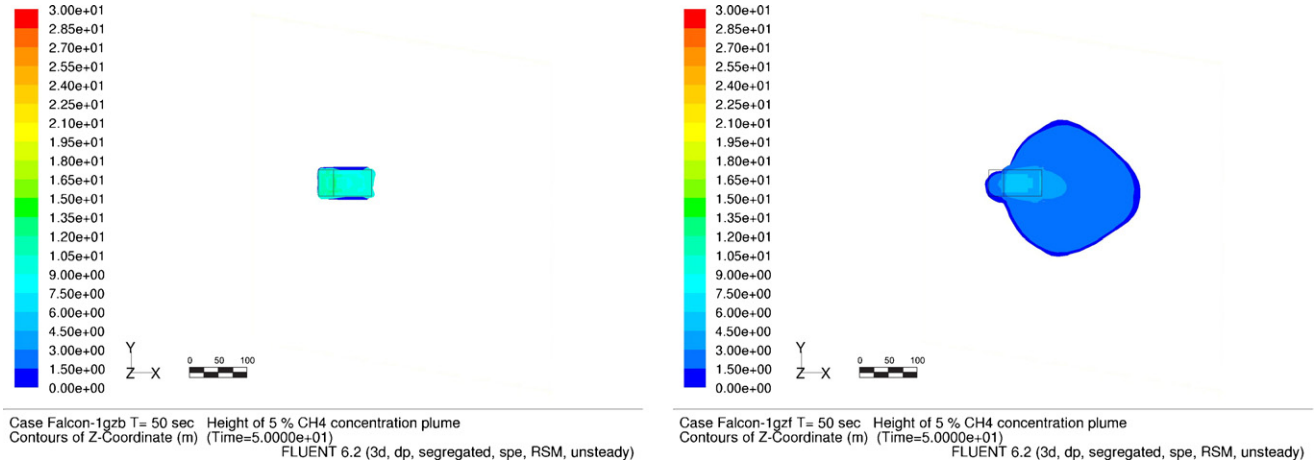

Fig. 11. Footprint of the flammable vapor cloud 50 s after the start of the spill (left = baseline case, right = no-barrier case).

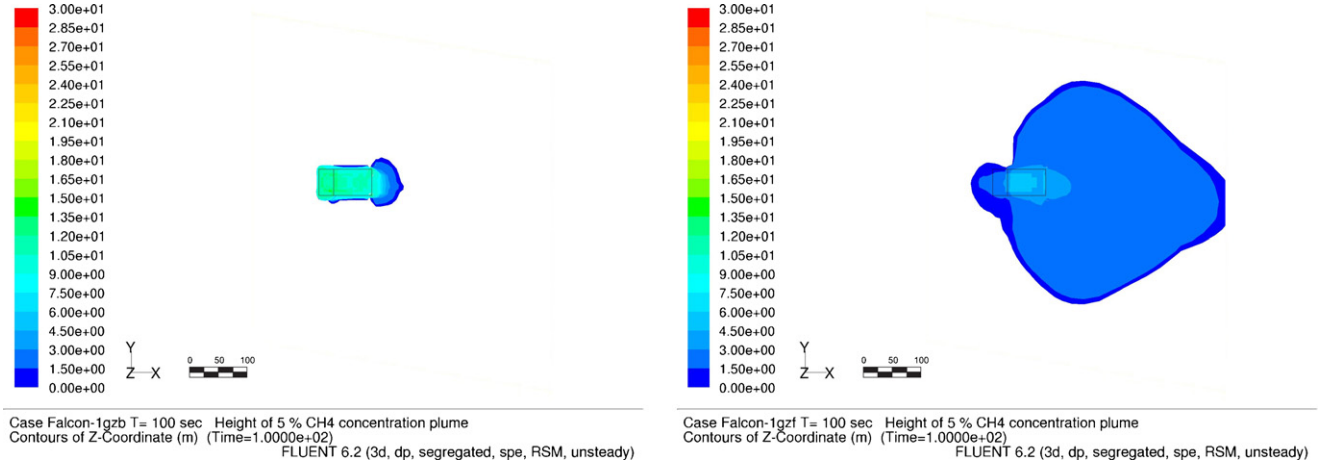

Fig. 12. Footprint of the flammable vapor cloud 100 s after the start of the spill (left = baseline case, right = no-barrier case).

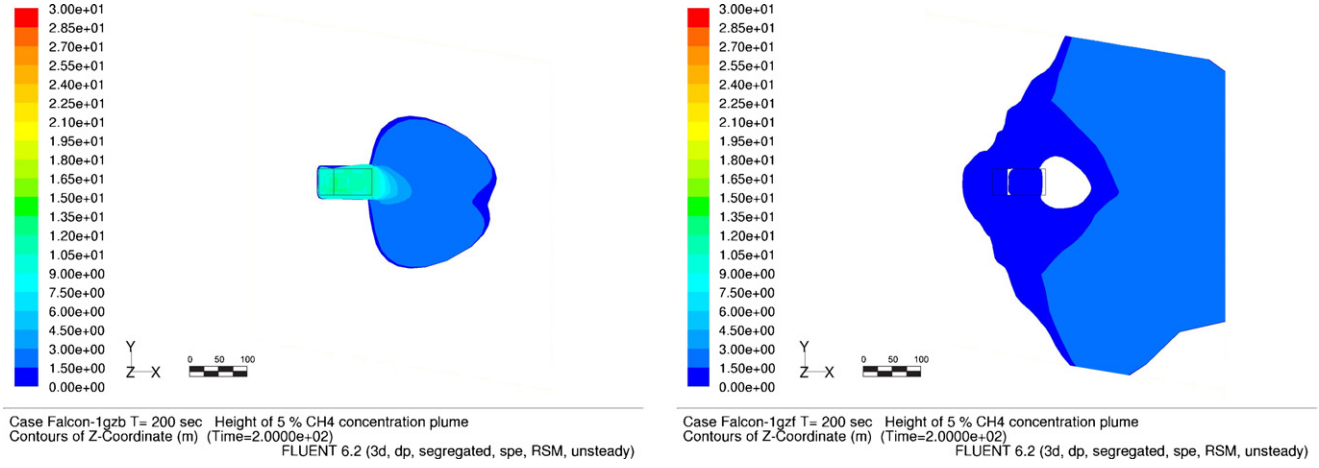

Fig. 13. Footprint of the flammable vapor cloud 200 s after the start of the spill (left = baseline case, right = no-barrier case).

downwind, whereas the confined cloud persists in the immediate proximity of the impoundment until the gas is dissipated. In the absence of impoundment the ignitable cloud has a markedly larger reach. Conversely, the impoundment serves a significant role in reducing the size of the ignitable cloud.

5.4. *Effects of source turbulence*

Wind blowing over the vapor fence and billboard generates turbulence, which is visualized in Fig. 15 in terms of turbulent kinetic energy (TKE) along a plane through the center of the

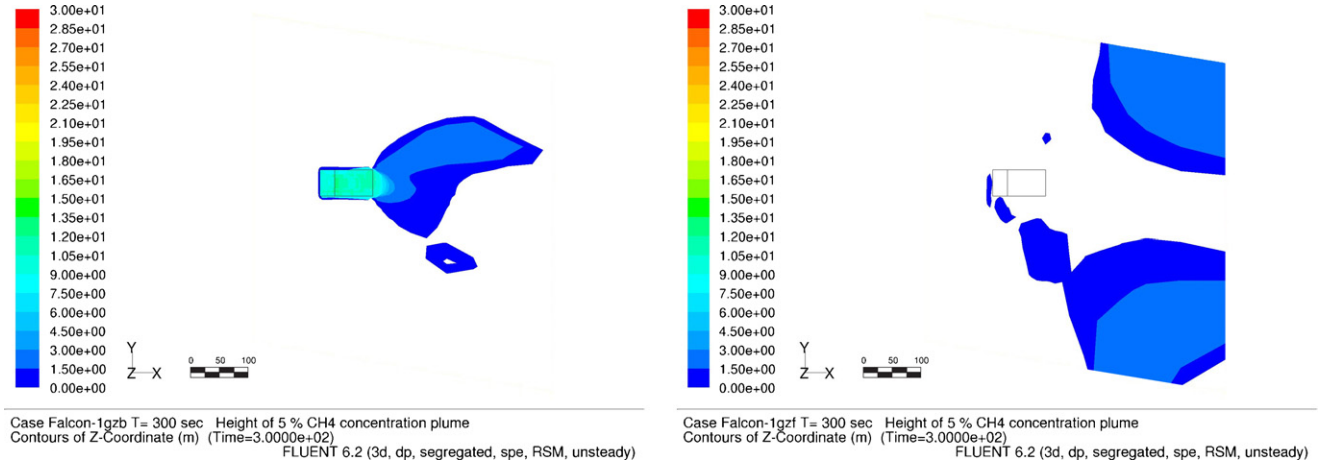

Fig. 14. Footprint of the flammable vapor cloud 300 s after the start of the spill (left = baseline case, right = no-barrier case).

impoundment. The peak TKE for the Falcon-1 Fluent simulation, prior to the injection of LNG, is slightly less than 1 m^2/s^2 for this low wind condition of 1.7 m/s at 2 m elevation and occurs in the wake of the billboard and of the downwind fence. The TKE gradually decreases with distance from the shear layer.

As discussed earlier, the Falcon test videos reveal that the LNG injection and evaporation process introduces turbulence at the area of injection, which allows the dense gas cloud to mix with air and to rise more rapidly inside the fence that undiluted saturated vapor would. The magnitude of the estimated TKE of 9 m^2/s^2 associated with the injection process was found to be large compared to the level of turbulence in the wake of the impoundment and billboard structures and is expected to control the mixing of gas vapor with air under low wind conditions. In order to assess the significance of the source turbulence on the vapor dispersion scenario, a comparison was made between the baseline case (TKE = 9 m^2/s^2 at the area of injection) and the same scenario without source turbulence (TKE = 0 m^2/s^2 at the area of injection).

Figs. 16 and 17 show, respectively, contours of TKE and gas concentration plotted on the center plane, 100 s after the start of the spill. The images on the left represent the baseline case, the images on the right represent the no-source-turbulence case. Fig. 17 shows that, without LNG source turbulence, the cold gas cloud remains highly stratified and undiluted with air within the impoundment. This limits the amount of natural gas that is entrained out of the impoundment by the much lesser turbulence associated with the wind. In contrast, the presence of source turbulence mixes air with the injected gas and dilutes its concentration within the impoundment. This process much more closely resembles the Falcon spill video.

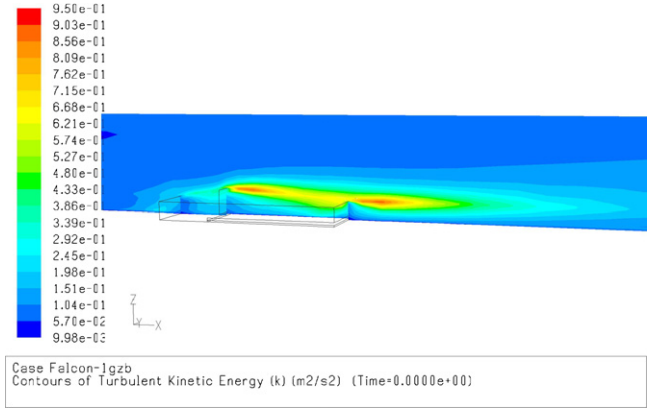

Fig. 15. Centerline turbulence intensity (TKE) before spill.

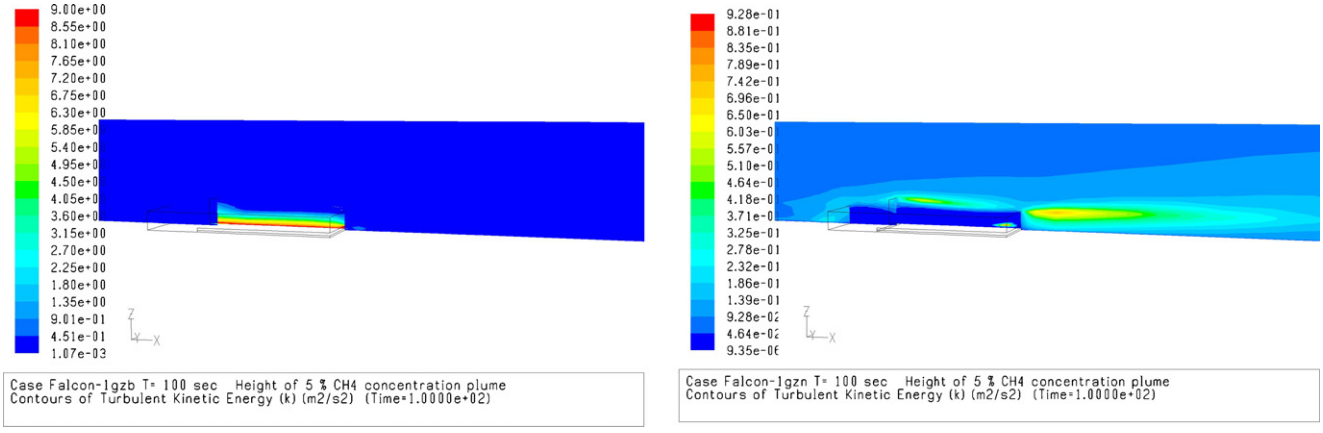

Fig. 16. Centerline TKE, 100 s into spill: with (left) and without (right) source turbulence (note the different TKE scales).

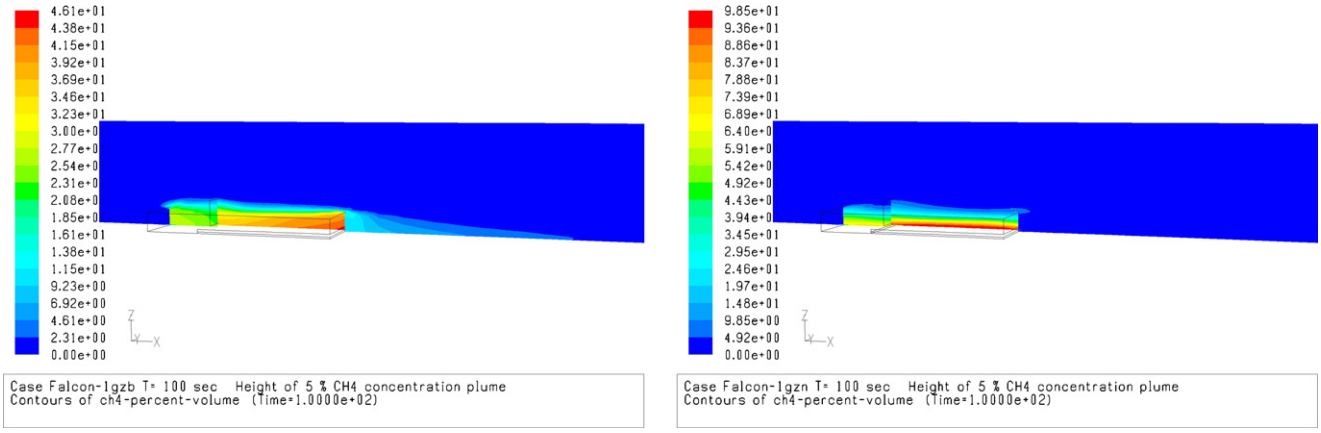

Fig. 17. Centerline gas concentration, 100 s into spill: with (left) and without (right) source turbulence.

In Fig. 16 (left), the source TKE of 9 m^2/s^2 at the pond surface decreases to approximately 1 m^2/s^2 at the top of the impoundment. In contrast, in Fig. 16 (right) the maximum TKE occurs at the top of the impoundment, where turbulence is generated by the wind shear layer, albeit at a much lower level for this low wind condition. In both cases the TKE decreases rapidly with distance away from its source. In a previous analysis, Chan [14] simulated the Falcon tests using a fixed diffusivity imposed within and near the fence enclosure. The diffusivity imposed in this region was the sum of a component based on the diffusivity of air and one based on the injected vapor velocity. Chan's approach echoes the need for a method to quantify the turbulence within the impoundment.

6. Conclusions

The simulations show that CFD can reproduce the experimental results from the Falcon tests with reasonable accuracy: at a distance of 150 m, the elevation of the ignitable cloud was between 5 and 6 m. The simulations showed that mixing and entrainment of gas caused by wind, under the low-wind and stable atmospheric conditions is small. Under the conditions of the Falcon-1 test, the turbulence generated by the spill and vaporization of LNG dominates the rate of mixing of the evaporated gas with air in the impoundment. In the extreme case of no source-turbulence, it was shown that the wind-induced turbulence would not be sufficient to generate sufficient mixing to cause the cold vapor cloud to overflow the impoundment.

The turbulence-driven entrainment of air and dilution of vaporized gas greatly affects the rate at which the diluted natural gas cloud grows within the impoundment and is dispersed out of it. It also influences the concentrations in the cloud downwind of the impoundment. Therefore, accurate representation of the LNG spill requires not only the knowledge of mass flow and evaporation rates, but also an estimate of the velocity at which the LNG is spilled and evaporated. The latter is essential to estimate the turbulent kinetic energy associated with the spill and its propensity to entrain air.

The vapor fence was shown to have a significant effect on reducing the flammable vapor cloud dispersion distance. The rate of spillage of gas out of impoundment is significantly lower than the spill rate itself, and the small exterior vapor cloud was found to remain attached to the impoundment wall. In the absence of impoundment, the vapor cloud is convected downwind causing ignitable vapors to travel significantly larger distances.

The Falcon tests were LNG spills on water, and not onto solid ground as would be the case in the event of spills into impoundments at onshore LNG facilities. The main difference between the two scenarios, however, is in the rate of LNG vapor generation over time: a spill onto solid ground would result in a rapidly decreasing LNG vapor generation rate, as the ground is progressively cooled down by the LNG pool, whereas a spill onto water (as in the Falcon tests) would result in an approximately constant LNG vapor generation rate, as convective motion within the water body would maintain the surface at approximately constant temperature. The lower vapor generation rate of a spill onto solid ground, however, does not affect the impoundment's vapor holdup capability. As a result, a significant reduction in vapor dispersion distance would be achieved in the event of a spill onto solid ground as compared to the observations shown here of an impoundment surrounding a spill on water.

This study also demonstrated that source-level turbulence, not wind-induced turbulence, is the dominating factor leading to the vapor cloud overflowing the impoundment. Source-level turbulence for a spill onto solid ground is expected to be smaller than for a spill onto water. Therefore, the reduction in vapor cloud dispersion for a spill onto solid ground, in an impoundment, can be expected to be greater than the reduction for the same spill onto water, in the same impoundment.

Additional work is in progress to validate Fluent using the Falcon tests. This effort will provide the industry with a widely available tool to accurately quantify the exclusion zones associated with LNG storage and processing areas.

References

[1] J. Havens, A Dispersion Model for Elevated Dense Gas Jet Chemical Releases, Volume 1, EPA-450/4-88-006a, 1998.
[2] FERC Docket No. CP05-396-000 and FERC Docket No. CP04-411-000.

[3] M. Hightower, et al., Guidance on Risk Analysis and Safety Implications of a Large Liquefied Natural Gas (LNG) Spill Over Water, Sandia National Laboratories Report: SAND2004-6258, December 2004.
[4] T.C. Brown, et al., Falcon Series Data Report 1987 LNG Vapor Barrier Verification Field Tests, Gas Research Institute Report GRI-89/0138, Contract 5085-252-1189, June 1990.
[5] W. Tang, et al., Application of CFD simulations for short-range atmospheric dispersion over open fields and arrays of buildings, in: AMS 14th Joint Conference on the Applications of Air Pollution Meteorology with the A&WMA, Atlanta, GA, January 30–February 2, 2006.
[6] C. Savvides, V. Tam, D. Kinnear, Dispersion of Fuel in Offshore Modules: Comparison of Predictions Using FLUENT and Full-Scale Experiments, Major Hazards Offshore, ERA, 2001.
[7] R.P. Cleaver, G.Y. Buss, V. Tam, S. Connolly, R.E. Britter, Analysis of Gas Build-Up from High Pressure Natural Gas Releases in Naturally-Ventilated Offshore Modules, 7th Annual Conference on Offshore Installations: Fire and Explosion Engineering, Church House Conference Centre, London, ERA report 98-0958, December 2, 1998.
[8] R.P. Cleaver, S. Burgess, G.Y. Buss, C. Savvides, S. Connolly, Analysis of gas build-up from high pressure natural gas releases in naturally-ventilated offshore modules, in: Eighth Annual Conference on Offshore Installations: Fire and Explosion Engineering, Church House Conference Centre, London, ERA, November 30, 1999.
[9] B.E. Launder, D.B. Spalding, The numerical computation of turbulent flows, Comput. Methods Appl. Mech. Eng. 3 (1974) 269–279.
[10] M.M. Gibson, B.E. Launder, Ground Effects on Pressure Fluctuations in the Atmospheric Boundary Layer, J. Fluid Mech. 86 (1978) 491–511.
[11] A. Luketa-Hanlin, A review of large-scale LNG spills: experiments and modeling, J. Hazard. Mater. A132 (2006) 119–140.
[12] R.P. Koopman, Data and Calculations on 5 m3 LNG Spill Tests, Laurence Livermore National Laboratory Report UCRL-52976, 1978.
[13] Fluent User's Manual, v. 6.2.
[14] S.T. Chan, Numerical simulations of LNG vapor dispersion from a fenced storage area, J. Hazard. Mater. 30 (1992) 195–224.